PV PERFORAMNCE DURING LOW IRRADIANCE AND RAINY WEATHER CONDITIONS

Kendall B.D. Esmeijer, Atse Louwen, Wilfried G.J.H.M. van Sark
Utrecht University, Copernicus Institute of Sustainable Development
Heidelberglaan 2, 3584 CS Utrecht, the Netherlands

ABSTRACT: With data made available by a photovoltaic (PV) test facility located on top of an office building of the Utrecht University the performance of ten PV modules during time periods of low irradiance and precipitation was analysed. Using values for direct irradiance by Bird's SPCTRAL2 model and measured climatic conditions a weather classification system was designed in order to categorize time periods and make a comparison between rainy and non-rainy time periods possible. Results show that precipitation induces a blue shift in the solar spectrum increasing the short-circuit current (I_{SC}) of the modules (a-Si and CdTe in particular). Furthermore it is shown that precipitation causes module temperature to drop resulting in an increase in open-circuit voltage (V_{OC}) for all modules. In terms of the performance ratio (PR) it is shown that almost all modules perform better under rainy than under non-rainy weather conditions, but it is noted that incorrect measurements of module temperature most likely overestimate the PR for some of the investigated modules.
Keywords: Performance, Environmental effect, Rain, a-Si

1 INTRODUCTION

The performance of photovoltaic (PV) modules is generally measured indoors under standard test conditions (STC) of 25 °C module temperature and an AM1.5 broadband irradiance of 1000 W m-2. Under outdoor weather conditions this standard is however rarely met. Under cloudy weather conditions for instance the spectrum of downwelling irradiance differs from that under clear sky conditions [1]. In the Netherlands there are few hours a year in which there are no clouds present. Furthermore time periods in which precipitation is measured are also not uncommon in the Netherlands [2]. Literature focussing on PV performance during time periods of precipitation is, to our knowledge, non-existent. Research was therefore conducted towards ascertaining the performance of different commercially available PV modules under low irradiance and rainy weather conditions.

The effects of precipitation were determined by comparing performance under low irradiance and rain with those under low irradiance and no rain. Differences in physical module properties and climatic conditions during both weather conditions were analysed in order to identify possible drivers for performance enhancement/impedance.

A novel weather classification system was developed with the use of indices for cloud cover identification from previous studies. This system was used to distinguish between certain weather conditions and served as a tool to select and group data to be analysed.

The data used in this work was made available by the Utrecht Photovoltaic Outdoor Test facility (UPOT) which collects performance data of several PV modules spanning the full range of today's commercially available PV modules as well as weather data [3].

2 METHODS

2.1 Performance measurements

Apart from using the module specific I_{SC} and V_{OC} as indicators for module performance the PR was used in order to make a comparison between different module types possible. It corrects for performance under non-STC conditions including plane of array irradiance (H_{POA}) and module temperature (T_{module}) [4]. The PR is a dimensionless measure of module performance given by;

$$PR = E_{specific}/H_{specific} * 100\% \quad \textbf{(1)}$$

$$E_{specific} = E_{feed-in}/P_{STC} \quad \textbf{(2)}$$

$$H_{specific} = H_{POA}/G_{STC} \quad \textbf{(3)}$$

$$E_{feed-in} = P_{mp} * \left(1 + \gamma_{mp} * (T_{module} - T_{STC})\right) \quad \textbf{(4)}$$

Here, P_{STC} and G_{STC} refer to power output and total irradiance under STC. $E_{feed-in}$ stands for the measured power output. The negative temperature coefficient is represented by γ_{mp} and T_{STC} refers to a module temperature of 25℃.

2.2 Module responsivity

The efficiency with which a material is capable of allowing photons of a certain wavelength to create an electron-hole pair is referred to as the Internal Quantum Efficiency (IQE) and is wavelength specific [5];

$$IQE(\lambda) = \frac{\#\ of\ electron-hole\ pairs}{\#\ of\ incident\ photons(\lambda)} \quad \textbf{(5)}$$

With a plot of IQE set out against wavelength, the responsiveness of a solar module to certain ranges of spectral radiation can be made insightful. This is done in Fig. 1 for typical PV modules made of different semiconductor materials [6]. The figure shows that for some technologies the spectral response is narrow in the region of short wavelength/high energy photons (e.g. a-Si and CdTe). Other technologies have a broader response across a larger range of photon wavelengths/energies (e.g. CIS, CIGS and c-Si). Of course short/long and low/high here are relative to the chosen ranges.

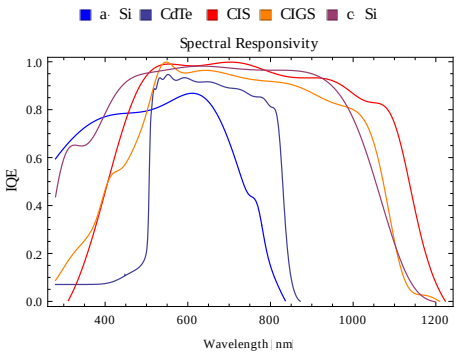

Figure 1: Spectral responsivity of different typical photovoltaic modules in terms of the internal quantum efficiency over a wavelength range

2.3 Spectral characterization

Using the spectral irradiance at every individual wavelength to characterize the spectral distributions under certain weather conditions would however require laborious efforts to be taken. Instead, a single index of Average Photon Energy (APE) can be used as a good indicator of spectral variation [7, 8]. The APE is defined as the average energy per photon which is included in the analysed spectrum and is calculated by division of the integrated irradiance (E(λ)dλ) over the integrated photon flux density (Φ(λ)dλ);

$$APE = \frac{\int_a^b E(\lambda)d\lambda}{q\int_a^b \Phi(\lambda)d\lambda} \quad \textbf{(6)}$$

Here, q represents the electron charge ($1.602*10^{-19}$ C) used for unit conversion from J to eV, and a and b are arbitrary wavelengths. The visible spectrum changing from blue to red as photon energy decreases leads to high values for APE corresponding to a "blue-rich" spectrum and low values for APE corresponding to a "red-rich" spectrum at equal broadband irradiance. The wavelength range used in this work is 350-1050 nm.

2.4 Experimental setup

The test facility is located on the rooftop of the eight storey Hans Freudenthal building of the Utrecht University (52.09°N, 5.17°E). It was designed for the purpose of assessing the performance of 12 commercially available PV modules under outdoor weather conditions. Two types of each module were installed and connected to the two separate inverters (channel 1 and channel 2). The modules investigated in this study (10 in total) are made from different materials; mono-Si (three types), poly-Si (two types), a-Si, CdTe, CIGS, HIT and CIS.The setup is positioned according to the solar azimuth and plane of array angles of 180° and 37° respectively.

With the exemption of the weather station, which is fabricated by Lufft GmbH, all measuring equipment (pyranometers, spectroradiometer, sun tracker and a pyrheliometer) are designed by EKO Instruments [9, 10]. Both in-plane and horizontal irradiance measurements as well as weather measurements are being performed on a one minute interval. Module performance measurements have a three minute resolution and are performed at irradiance levels exceeding 50 Wm^{-2}. The measurements of the in-plane irradiance are synchronized with those of the module performance. The setup is shown in Fig. 2.

Figure 2: Picture of UPOT on a clear sky day

Construction work on the terrain of the University Utrecht resulted in a large construction crane being position south of the test facility, directly in front of the Hans Freudenthal building. The end of the crane being able to move straight over the test facility and the base being positioned right in front of it resulted in frequent shadows being casted over the modules and measuring equipment. The range of data used in this work is 2013-03-20 to 2013-11-05 and is bound by the installation of the pyrheliometer and the positioning of the construction crane.

2.5 Weather classification

Cloud cover is often measured in oktas which depend on a visual interpretation of the sky. Given the laborious effort it would require to interpret cloud cover on this scale for every timestamp (performance and irradiance measurements have a granularity of a few seconds) a cloud cover classification system has been implemented which uses physical properties as inputs. The system uses the clearness index and the variability index, as proposed by Stein et al., to give a representation of the cloud cover [11]. Both these parameters are calculated based on irradiance values during a clear sky day. For this purpose the SPCTRAL2 clear sky model has been used which estimates both direct and diffuse irradiance [12]. Given the lack of accurate inputs which are needed for the calculation of the diffuse component, the modelled irradiances presented in this work refer to the direct component only.

The clearness index is a parameter which indicates the irradiance intensity. It gives the ratio between the measured direct irradiance $I_{D,meas,t}$ during a certain time interval T and the modelled direct irradiance $I_{D,mod,t}$ during the same interval and is given by;

$$CI = \frac{\sum_{t=1}^{T} I_{D,meas,t}}{\sum_{t=1}^{T} I_{D,mod,t}} \quad \textbf{(7)}$$

Fig. 3 shows a day in which CI for most time intervals would have a value of 1.

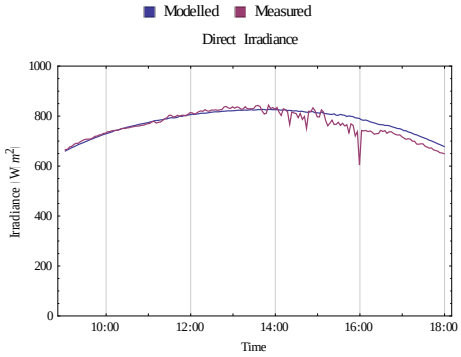

Figure 3: Example of a day on which the value for CI is near unity for the entire day (2013-06-07)

The variability index is a parameter which indicates the irradiance variability. It was first proposed by Stein et al. and can be conceived conceptually as the ratio between two lines; the "length" of $I_{D,meas}$ plotted against time and the "length" of $I_{D,mod}$ plotted against time. It is given by;

$$VI_{Stein\ et\ al.} = \frac{\sum_{k=1}^{n}\sqrt{\left(I_{D,meas,k}-I_{D,meas,k-1}\right)^2+\Delta t^2}}{\sum_{k=1}^{n}\sqrt{\left(I_{D,mod,k}-I_{D,mod,k-1}\right)^2+\Delta t^2}} \quad \textbf{(8)}$$

The iterator k and k-1 represent consecutive measurements taken in the time interval Δt. This variability index has been adjusted in two manners. First, seeing as the representation of cloud variability by means of the "length" of two lines has no physical meaning (i.e. $\sqrt{\left(\frac{W}{m^2}\right)^2+s^2}$ is not a physical unit) the variability index used in this work is adjusted to exclude the time component. Second, dividing the absolute differences in irradiance would yield very high values for days with partial cloud cover making comparisons between different days difficult. The square root of the ratio is therefore taken in order to group the extreme values and maintain a distinction between days in which the variability in irradiance is relatively low. The variability index used therefore becomes;

$$VI = \sqrt{\frac{\sum_{k=1}^{n}\left(I_{D,meas,k}-I_{D,meas,k-1}\right)}{\sum_{k=1}^{n}\left(I_{D,mod,k}-I_{D,mod,k-1}\right)}} \quad \textbf{(9)}$$

Fig. 4 shows a day in which VI for most time intervals would have a relatively high value.

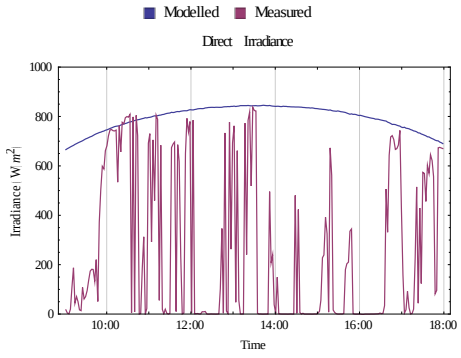

Figure 4: Example of a day on which the value for CI is high for the entire day (2013-05-24)

2.6 Data selection

The selection of time periods to be added to the dataset has eventually been done using three parameters: H_{POA} (<250 Wm^{-2} for at least two consecutive hours), cloud cover type (overcast/low values for CI and VI) and precipitation (measured or not measured). The dataset consists of approximately 2000 measurements.

3 RESULTS

3.1 Effect on physical module properties and climatic conditions

3.1.1 Effect on module temperature

In Fig. 5 (a) $T_{ambient}$ is accounted for, by selection of hours in which $T_{ambient}$ remains constant, and it illustrates that as the precipitation intensity increases, T_{module} decreases and that this is not caused by a decrease in $T_{ambient}$.

In Fig 5 (b), which pertains to the same timeperiod as in (a), H_{POA} is accounted for and it is illustrated that in periods of relatively low to no precipitation T_{module} is driven by H_{POA} and that this mechanism is reduced in periods of increased precipitation intensity.

Fig. 6 (a) and (b) represent a different timeperiod in which wind speed remains fairly constant and T_{module} increases in the hours in which no precipitation was measured. These observations indicate that rainfall lowers T_{module} despite any other climatic conditions. The measurements presented in Fig. 5 and Fig. 6 pertain to those recorded for the CdTe module. The cooling effect of precipitation was however noticed for all modules.

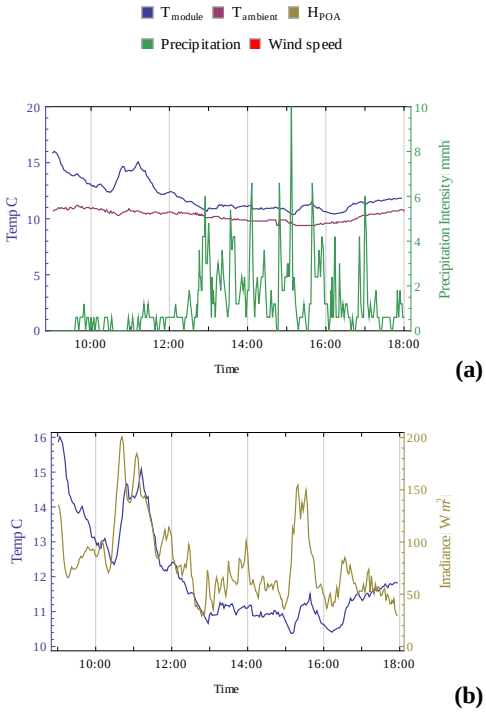

Figure 5: The effect of precipitation on module temperature when accounting for $T_{ambient}$ and irradiance

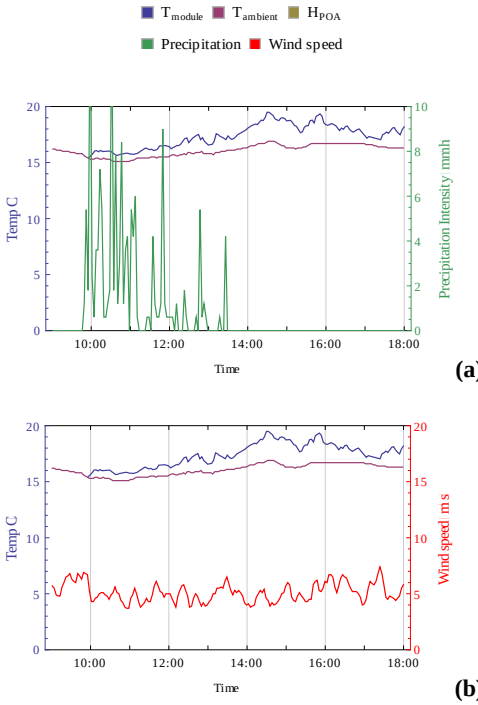

Figure 6: The effect of precipitation on module temperature when accounting for $T_{ambient}$ and wind speed

3.1.2 Effect on spectrum

Fig. 7 shows that precipitation changes the composition of spectral irradiance in terms of the distribution in recorded APE values. It indicates that precipitation causes the spectrum to shift towards the blue (high values for APE).

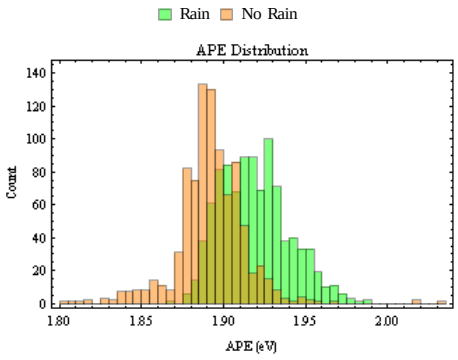

Figure 7: Distribution in APE values for rainy and non-rainy timeperiods

Fig. 8 relates this shift in spectral irradiance to the spectral responsivity of some typical solar modules. It is shown that the mean APE is higher during rainy (green line) than during non-rainy (orange line) time periods. The non-vertical lines show that, in the investigated region, the IQE increases for the a-Si and CdTe modules and that for the other modules the IQE remains fairly constant.

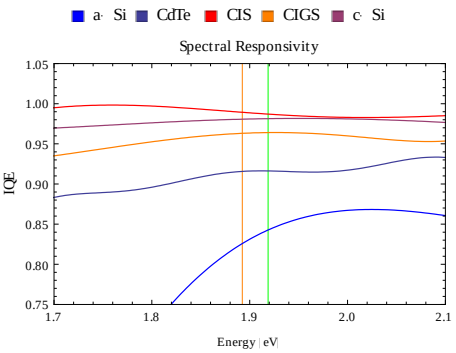

Figure 8: Mean APE values set out against the spectral responsivity of some typical modules

3.1.3 Effect of precipitation intensity

In Fig. 9 (a) and (b) H_{POA} is set out against I_{SC} for the three time periods with different precipitation levels. The a-Si module is presented here because of its presumed higher sensitivity to changes in the spectral composition and the mono-Si B module is presented because its performance, in terms of I_{SC} and V_{OC}, correspond to that of most of the other investigated modules. It can be seen that the intensity differences do not result in significant changes in I_{SC} (the regression lines overlap). This shows that, other than through a change in the spectral irradiance and the total irradiance, precipitation intensity has no clear effect on I_{SC}.

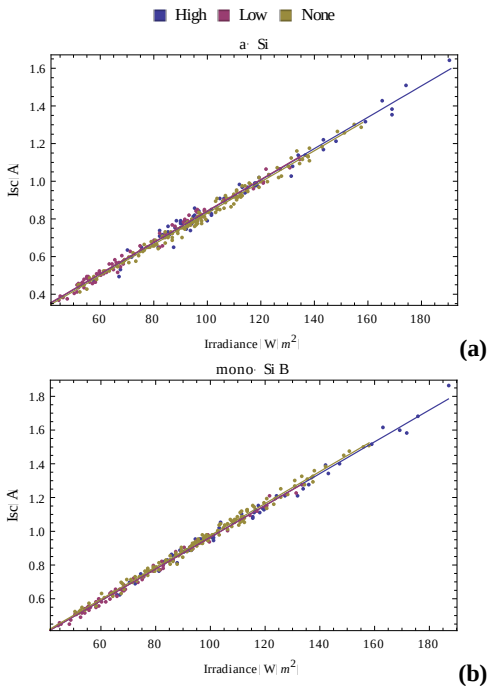

Figure 9: Temperature corrected values for I_{SC} set out against H_{POA} under equal levels of mean APE and three different levels of precipitation for the a-Si module

3.2 Effect on performance

3.2.1 Effect on short circuit current

As is expected from the observations from Fig. 8 the a-Si (and also) CdTe modules under rainy weather conditions outperform those under non-rainy weather conditions. This is shown in Fig. 10 (a). What is striking

though is that the other modules, which according to Fig. 8 should not be as sensitive to changes in the spectrum, also perform slightly better under rainy weather conditions. This is shown in Fig. 10 (b). It should be noted that the spectral responsivity curves shown earlier pertain to typical modules for each technology. The specific responsivity of the investigated modules could therefore be such that they, just like the a-Si and CdTe modules, perform better under rainy weather conditions in which the APE is generally higher. This could then explain the difference in I_{SC} performance between the two weather conditions. If not then there is some other undefined mechanism which results in this difference.

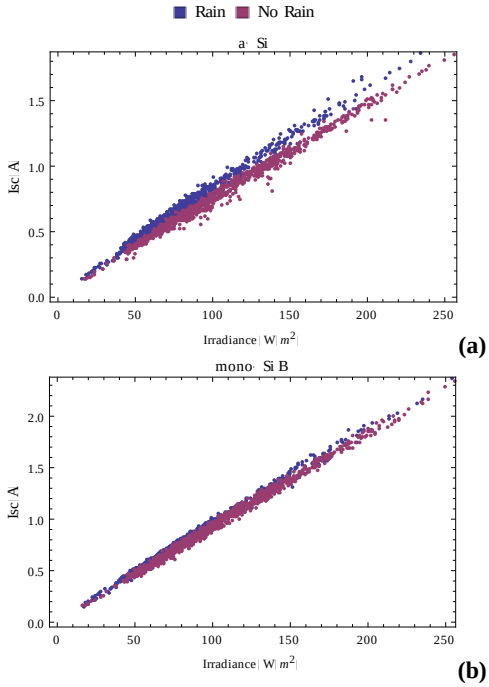

Figure 11: Temperature corrected values for I_{SC} set out against H_{POA} under rainy and non-rainy time periods.

3.2.2 Effect on open circuit voltage

The effect of precipitation of V_{OC} is shown in Fig. 12 (a) and (b) for the same modules as presented in the previous sections. If the applied temperature coefficients are accurate and no other major mechanisms are at play then the data points in these plots should lay on the same regression line. Fig. 12 however clearly shows that the rainy data points lay above the non-rainy data points. A plausible explanation for this observation is that the temperature measurements are inaccurate because of a delay in temperature change. The temperature sensor is located on the back side of each solar module. The thermal conductivities of the different materials comprising the module are such that changes in temperature occurring at the front end, due to precipitation, will not immediately result in a drop in temperature at the back where the sensor is positioned. This delay in temperature drop will mean that recorded temperatures are too high and subsequently result in temperature corrections being too severe (i.e. the rainy data points are too high).

What can furthermore be seen in Fig. 13 is that the difference in rainy and non-rainy V_{OC} for the a-Si and CdTe modules is significantly higher than the difference for the other modules. Recalling the observed increase in I_{SC} during rainy time periods from the previous section explains this residuary non-congruent pattern in V_{OC}.

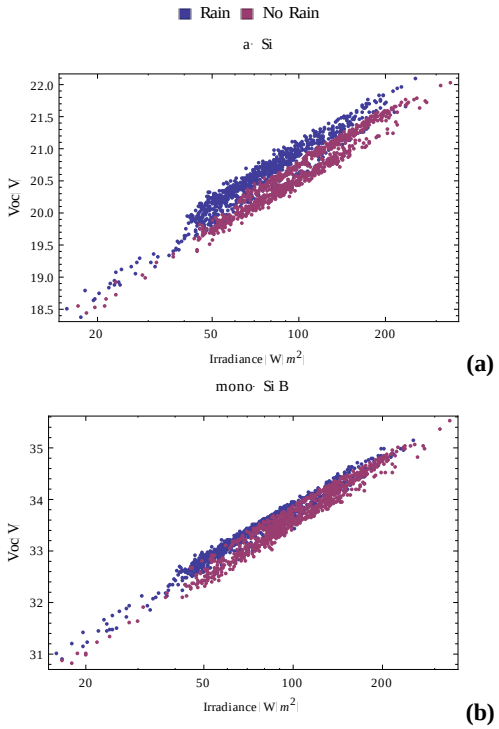

Figure 12: Temperature corrected values for V_{OC} (logarithmic scale) set out against H_{POA} under rainy and non-rainy time periods

3.2.3 Effect on performance ratio

The difference in PR under rainy and non-rainy weather conditions for each of the investigated modules is shown in Fig. 13 where PR calculations pertain to mean values of both datasets ($\Delta PR = PR_{rain}-PR_{no\ rain}$). If the results for the poly-Si A and CIS modules are neglected the ΔPR values for all other modules can be understood from a consideration of the previous results; a) all modules have a slightly higher V_{OC} during rainy weather periods, due to a delay in recorded temperature drop, resulting in ΔPR of a few percent for all modules and b) the a-Si and CdTe modules have a higher I_{SC} and V_{OC} during rainy weather conditions due to changes in the spectral irradiance resulting in even higher values for their ΔPR.

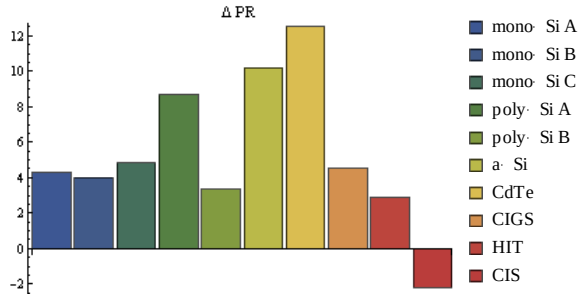

Figure 13: Difference between rainy and non-rainy PR for all investigated modules

The poly-Si A and CIS modules performing different than expected is also made apparent when looking at the

distribution in ΔPR in Fig. 14 (a) and (b). The PR distribution under non-rainy weather conditions is broad and the mean and mode values for PR are different (e.g. there is no clear bell shaped distribution). The majority of recorded non-rainy PR's furthermore are a lot lower than those of the other modules. For the CIS module it is striking that although the distributions are near normal the peaks of both the rainy and non-rainy PR's are relatively low. The absolute PR's are therefore also lower. These observations give rise to the assumption that these specific modules are faulty and that their performance can't be used as a technology specific benchmark.

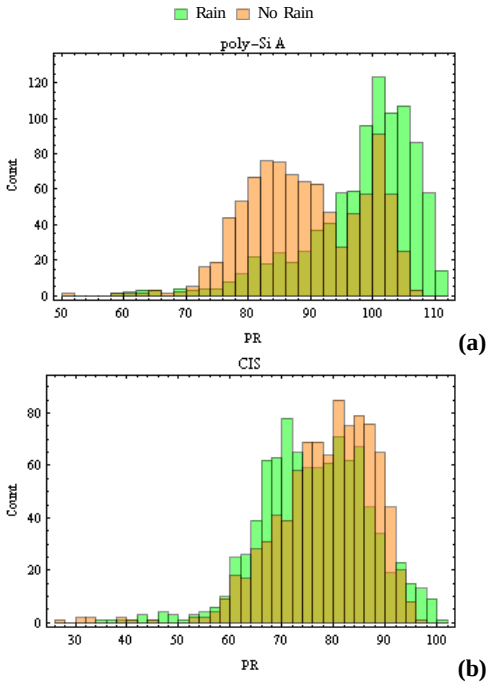

Figure 14: Distribution in PR during rainy and non-rainy time periods

4 CONSLUSIONS

The results show that, although there is discrepancy between technologies, with the exemption of the CIS module all investigated PV modules, operating under low irradiance levels, have a higher performance during rainy than under non-rainy weather conditions. Precipitation causes module temperatures to drop resulting in increased open circuit voltage. At low irradiance levels precipitation furthermore seems to shift the spectral irradiance more towards the blue resulting in short circuit current to increase for modules which have a higher spectral responsiveness in this region. The combined performance enhancement, given in terms of PR, showed that precipitation can increase performance by up to more than 12%. It should however be noted that part of this increase might be caused by measurement inaccuracies. Temperature corrections for instance are applied to account for losses in V_{OC} caused by measured T_{module} rising above STC T_{module}. Measured T_{module} at the back end is likely higher than that at the front end where incident photons excite electrons, espicially at the onset of precipitation. Deviations from STC temperature are therefore too high resulting in temperature corrections being too high as well. As a result presented temperature corrected PR values attribute too much difference between rainy and non-rainy PR's to a shift in spectral irradiance. Accounting for this still yields significantly higher PRs for a-Si and CdTe modules during rainy weather conditions.

5 REFERENCES

[1] Barlett J, Ciotti A, Davis R, Cullen J. *The spectral effects of clouds on solar irradiance*. Journal of Geophysical Research (1998) 31,017-31,031

[2] KNMI, http://www.knmi.nl/klimatologie/uurgegevens/selectie.cgi

[3] van Sark W.J.G.H.M., Louwen A, de Waal A, Elsinga B, Schropp R. E.I. *UPOT: The Utrecht photovoltaic outdoor test facility*. 27th EU PVSEC, Frankfurt, Germany 2012

[4] N. H. Reich, B. Mueller, A. Armbruster, van W. G. J. H. M. Sark, K. Kiefer, and C. Reise. *Performance ratio revisited: is pr > 90 % realistic?*, Progress in Photovoltaics: Research and Applications 2012; 20:717–726

[5] Honsberg C, Bowden S. *PVCDROM*, http://pveducation.org/pvcdrom

[6] ten Kate O.M., Personal communication, 2014-02-11

[7] Minemoto, T., Toda, M., Nagae, S., Gotoh, M., Nakajima, A., Yamamoto, K., Hamakawa, Y.. *Effect of spectral irradiance distribution on the outdoor performance of amorphous Si/thin-film crystalline Si stacked photovoltaic modules*. Solar Energy Materials and Solar Cells 2007; 91: 120-122

[8] Williams, S., Betts, T., Helf, T., Gottschalg, R., Beyer, H., & Infield, D.. *Modeling long-term module performance based on realistic reporting conditions with consideration to spectral effects*. Proceedings of the Third World Conference on Photovoltaic Energy Conversion, Osaka, Japan 2003

[9] EKO Instruments, http://eko-eu.com

[10] Lufft GmbH, http://www.lufft.com/en/

[11] Stein J. S., Reno M.J., Hansen C.W.. *The variability index: a new and novel metric for quantifying irradiance and PV output variability*. Sandia National Laboratories

[12] Bird R.E., Riordan C. *Simple solar spectral model for direct and diffuse irradiance on horizontal and tilted planes at the earth's surface for cloudless atmospheres*. Journal of climate and applied meteorology 1986; 25: 87-97